2018

Thermo-optic Tuning of a Packaged Whispering Gallery Mode Resonator Filled with Nematic Liquid Crystal

Vishnu Kavungal
Technological University Dublin, vishnu.kavungal@tudublin.ie

Gerald Farrell
Technological University Dublin, gerald.farrell@tudublin.ie

Qiang wu
Technological University Dublin, qiang.wu@tudublin.ie

Arun Mallik
Technological University Dublin, arun.mallik@tudublin.ie

Yuliya Semenova
Technological University Dublin, yuliya.semenova@tudublin.ie

Recommended Citation

Kavangul, V., Farrell, G. & Qiang, W. (2018). Thermo-optic tuning of a packaged whispering gallery mode resonator filled with nematic liquid crystal. *Optics Express*, vol. 26, no. 7, pp. 8431-8442. doi: 10.1364/OE.26.008431.

Research Article | Vol. 26, No. 7 | 2 Apr 2018 | OPTICS EXPRESS 8431
Optics EXPRESS

Thermo-optic tuning of a packaged whispering gallery mode resonator filled with nematic liquid crystal

VISHNU KAVUNGAL,[1,*] GERALD FARRELL,[1] QIANG WU,[1,2] ARUN KUMAR MALLIK,[1] AND YULIYA SEMENOVA[1]

[1]*Photonics Research Centre, Dublin Institute of Technology, Kevin St, Dublin, Ireland*
[2]*Department of Mathematics, Physics and Electrical Engineering, Faculty of Engineering and Environment, Northumbria University, Newcastle upon Tyne, NE1 8ST, UK*
[*]*vishnu.kavungal@mydit.ie*

Abstract: Thermo-optic tuning of whispering gallery modes (WGMs) in a nematic liquid crystal-filled thin-walled capillary tube resonator is reported. WGMs were excited by the evanescent field from a tapered optical fiber. Tapered optical fiber fabrication and reduction of wall thickness of the capillary tube was carried out by a ceramic micro-heater brushing technique. A simple and robust packaging technique is demonstrated to ensure stable and repeatable operation of the device. Tunability of WGMs with temperature was demonstrated with a sensitivity of 267.5 ± 2.5 pm/°C. The demonstrated thermo-optic method for WGMs tuning is potentially useful for many tunable photonic devices and sensors.

OCIS codes: (060.2370) Fiber optics sensors; (140.3945) Microcavities; (140.3948) Microcavity devices.

References and links

1. B. Matsko, A. A. Savchenkov, D. Strekalov, V. S. Ilchenko, and L. Maleki, "Review of applications of whispering-gallery mode resonators in photonics and nonlinear optics," IPN Progress Report **42**, 1–51 (2005).
2. V. S. Ilchenko and A. B. Matsko, "Optical Resonators with whispering-gallery modes—Part II: Applications," IEEE J. Sel. Top. Quantum Electron. **12**(1), 15–32 (2006).
3. J. D. Suter, I. M. White, H. Zhu, and X. Fan, "Thermal characterization of liquid core optical ring resonator sensors," Appl. Opt. **46**(3), 389–396 (2007).
4. N. Lin, L. Jiang, S. Wang, H. Xiao, Y. Lu, and H. L. Tsai, "Design and optimization of liquid core optical ring resonator for refractive index sensing," Appl. Opt. **50**(20), 3615–3621 (2011).
5. M. L. Gorodetsky and I. S. Grudinin, "Fundamental thermal fluctuations in microspheres," J. Opt. Soc. Am. B **21**(4), 697–705 (2004).
6. M. Han and A. Wang, "Temperature compensation of optical microresonators using a surface layer with negative thermo-optic coefficient," Opt. Lett. **32**(13), 1800–1802 (2007).
7. T. Carmon, L. Yang, and K. Vahala, "Dynamical thermal behavior and thermal self-stability of microcavities," Opt. Express **12**(20), 4742–4750 (2004).
8. A. B. Matsko, A. A. Savchenkov, N. Yu, and L. Maleki, "Whispering-gallery-mode resonators as frequency references. I. Fundamental limitations," J. Opt. Soc. Am. B **24**(6), 1324–1335 (2007).
9. A. A. Savchenkov, A. B. Matsko, V. S. Ilchenko, N. Yu, and L. Maleki, "Whispering-gallery-mode resonators as frequency references. II. Stabilization," J. Opt. Soc. Am. B **24**(12), 2988–2997 (2007).
10. I. Teraoka, "Analysis of thermal stabilization of whispering gallery mode resonance," Opt. Commun. **310**, 212–216 (2014).
11. A. Chijioke, Q.-F. Chen, A. Yu. Nevsky, and S. Schiller, "Thermal noise of whispering-gallery resonators," Phys. Rev. B **85**(5), 053814 (2012).
12. M. R. Foreman, W. L. Jin, and F. Vollmer, "Optimizing detection limits in whispering gallery mode biosensing," Opt. Express **22**(5), 5491–5511 (2014).
13. B. Guha, J. Cardenas, and M. Lipson, "Athermal silicon microring resonators with titanium oxide cladding," Opt. Express **21**(22), 26557–26563 (2013).
14. L. He, Ş. Kaya Özdemir, J. Zhu, and L. Yang, "Scatterer induced mode splitting in poly(dimethylsiloxane) coated microresonators," Appl. Phys. Lett. **96**(22), 221101 (2010).
15. J. Zhu, S. K. Ozdemir, L. He, and L. Yang, "Optothermal spectroscopy of whispering gallery microresonators," Appl. Phys. Lett. **99**(17), 171101 (2011).
16. L. He, Y.-F. Xiao, C. Dong, J. Zhu, V. Gaddam, and L. Yang, "Compensation of thermal refraction effect in high-Q toroidal microresonator by polydimethylsiloxane coating," Appl. Phys. Lett. **93**(20), 201102 (2008).

#313426 https://doi.org/10.1364/OE.26.008431
Journal © 2018 Received 14 Nov 2017; revised 19 Jan 2018; accepted 19 Jan 2018; published 23 Mar 2018

Optics EXPRESS

17. S. Lane, F. Marsiglio, Y. Zhi, and A. Meldrum, "Refractometric sensitivity and thermal stabilization of fluorescent core microcapillary sensors: theory and experiment," Appl. Opt. **54**(6), 1331–1340 (2015).
18. B. Özel, R. Nett, T. Weigel, G. S. Schweiger, and A. Ostendorf, "Temperature sensing by using whispering gallery modes with hollow core fibers," Meas. Sci. Technol. **21**(9), 094015 (2010).
19. C. H. Dong, L. He, Y. F. Xiao, V. R. Gaddam, S. K. Özdemir, Z. F. Han, G. C. Guo, and L. Yang, "Fabrication of high-Q polydimethylsiloxane optical microspheres for thermal sensing," Appl. Phys. Lett. **94**(23), 231119 (2009).
20. L. Shi, T. Zhu, D. Huang, and M. Liu, "Thermo–optic tuning of integrated polymethyl methacrylate sphere whispering gallery mode resonator," IEEE Photonics J. **8**(5), 2701307 (2016).
21. J. M. Ward, Y. Yang, and S. N. Chormaic, "Highly sensitive temperature measurements with liquid-core microbubble resonators," IEEE Photonics Technol. Lett. **25**(23), 2350–2353 (2013).
22. M. S. Nawrocka, T. Liu, X. Wang, and R. R. Panepucci, "Tunable silicon microring resonator with wide free spectral range," Appl. Phys. Lett. **89**(7), 071110 (2006).
23. B. B. Li, Q. Y. Wang, Y. F. Xiao, X. F. Jiang, Y. Li, L. Xiao, and Q. Gong, "On chip, high-sensitivity thermal sensor based on high-Q polydimethylsiloxane-coated microresonator," Appl. Phys. Lett. **96**(25), 251109 (2010).
24. S. H. Nam and S. Yin, "High-temperature sensing using whispering gallery mode resonance in bent optical fibers," IEEE Photonics Technol. Lett. **17**(11), 2391–2393 (2005).
25. V. R. Anand, S. Mathew, B. Samuel, P. Radhakrishnan, and M. Kailasnath, "Thermo-optic tuning of whispering gallery mode lasing from a dye-doped hollow polymer optical fiber," Opt. Lett. **42**(15), 2926–2929 (2017).
26. Y. Wu, Y. J. Rao, Y. H. Chen, and Y. Gong, "Miniature fiber-optic temperature sensors based on silica/polymer microfiber knot resonators," Opt. Express **17**(20), 18142–18147 (2009).
27. Y. Wang, H. Li, L. Zhao, Y. Liu, S. Liu, and J. Yang, "Tapered optical fiber waveguide coupling to whispering gallery modes of liquid crystal microdroplet for thermal sensing application," Opt. Express **25**(2), 918–926 (2017).
28. Z. Liu, L. Liu, Z. Zhu, Y. Zhang, Y. Wei, X. Zhang, E. Zhao, Y. Zhang, J. Yang, and L. Yuan, "Whispering gallery mode temperature sensor of liquid microresonastor," Opt. Lett. **41**(20), 4649–4652 (2016).
29. Y. Wang, H. Li, L. Zhao, Y. Liu, S. Liu, and J. Yang, "Tunable whispering gallery modes lasing in dye-doped cholesteric liquid crystal microdroplets," Appl. Phys. Lett. **109**(23), 231906 (2016).
30. H. C. Tapalian, J. P. Laine, and P. A. Lane, "Thermo-optical switches using coated microsphere resonators," IEEE Photonics Technol. Lett. **14**(8), 1118–1120 (2002).
31. I. M. White, H. Oveys, and X. Fan, "Liquid-core optical ring-resonator sensors," Opt. Lett. **31**(9), 1319–1321 (2006).
32. J. Wang, T. Zhan, G. Huang, P. K. Chu, and Y. Mei, "Optical microcavities with tubular geometry: properties and applications," Laser Photonics Rev. **8**(4), 521–547 (2014).
33. K. Yang and S. T. Wu, "*Fundamentals of liquid crystal devices*" (John Wiley & Sons, 2006).
34. J. N. Ptasinski, I. Khoo, and Y. Fainman, "Nematic Liquid Crystals for Temperature Stabilization of Silicon Photonics," in *Integrated Photonics Research, Silicon and Nanophotonics* (Optical Society of America, 2014), paper JT3A.20.
35. C.-L. Lee, H.-Y. Ho, J.-H. Gu, T.-Y. Yeh, and C.-H. Tseng, "Dual hollow core fiber-based Fabry-Perot interferometer for measuring the thermo-optic coefficients of liquids," Opt. Lett. **40**(4), 459–462 (2015).
36. S. J. Qiu, Y. Chen, F. Xu, and Y. Q. Lu, "Temperature sensor based on an isopropanol-sealed photonic crystal fiber in-line interferometer with enhanced refractive index sensitivity," Opt. Lett. **37**(5), 863–865 (2012).
37. M. Humar, "Liquid-crystal-droplet optical microcavities," Liq. Cryst. **43**(13-15), 1937–1950 (2016).
38. M. Sumetsky, R. S. Windeler, Y. Dulashko, and X. Fan, "Optical liquid ring resonator sensor," Opt. Express **15**(22), 14376–14381 (2007).
39. G. Brambilla, V. Finazzi, and D. Richardson, "Ultra-low-loss optical fiber nanotapers," Opt. Express **12**(10), 2258–2263 (2004).
40. W. Bogaerts, P. De Heyn, T. Van Vaerenbergh, K. De Vos, S. Kumar Selvaraja, T. Claes, P. Dumon, P. Bienstman, D. Van Thourhout, and R. Baets, "Silicon microring resonators," Laser Photonics Rev. **6**(1), 47–73 (2012).
41. A. Mahmood, V. Kavungal, S. S. Ahmed, G. Farrell, and Y. Semenova, "Magnetic-field sensor based on whispering-gallery modes in a photonic crystal fiber infiltrated with magnetic fluid," Opt. Lett. **40**(21), 4983–4986 (2015).
42. I. M. White and X. Fan, "On the performance quantification of resonant refractive index sensors," Opt. Express **16**(2), 1020–1028 (2008).
43. V. Kavungal, G. Farrell, Q. Wu, A. K. Mallik, and Y. Semenova, "A packaged whispering gallery mode strain sensor based on a polymer-wire cylindrical micro resonator," J. Lightw. Technol. in press).

1. Introduction

Optical whispering gallery modes (WGMs) are the electromagnetic resonances supported by open dielectric resonators with the dimensions in the order of few millimeters or smaller and a circular shape, e.g., spherical, cylindrical, disk, ring, toroidal etc. WGM resonances can be used in many applications, including optical sensors for biological and chemical compounds,

Optics EXPRESS

as electro-optical oscillators and modulators, all optical switches, tunable optical filters, or in quantum electro dynamic applications. The versatility of WGM resonators arises from their many advantages, such as high Q-factors, low mode volumes, and the exceptional sensitivity of the optical properties of the resonator to its size as well the nature of the surrounding medium [1, 2]. The exceptional sensitivity of the WGM resonators' optical properties to the changes in their geometry and refractive index may lead to significant temperature dependence due to thermos-optic and thermal expansion properties of the resonator's material.

Several authors reported different approaches to eliminate the temperature cross-sensitivity of sensors based on WGM resonators, such as liquid core optical ring resonators (LCORR) [3, 4], microspheres [5–12], micro ring [13], microtoroid [14–16] and fluorescent core micro capillary (FCM) [17], allowing to improve their performance. At the same time several studies reported applications of the temperature induced spectral shift in WGM resonators for temperature sensing or in tunable devices based on microspheres [18–20], microbubble [21], microring [22], microtoroid [23], bent optical fiber [24], dye doped hollow polymer optical fiber [25], microfiber knot resonator [26], and spherical droplets [27–29].

Silica glass is one of the most popular materials used for fabrication of optical WGM microresonators (MRs) due to its low loss and the simplicity of fabrication of high quality resonators by melting the material into circular shapes. However, silica has relatively low thermo-optic and thermal expansion coefficients, so if a silica resonator device is used for sensing of environmental parameters or utilizes thermo-optic tuning, a means to enhance its temperature sensitivity is required. Such an enhancement is often achieved by coating of the resonator surface with suitable functional materials. For example, authors in [30] used a conjugated polymer coated silica microsphere with an improved temperature sensitivity to design a thermo-optical switch. B. B. Li *et al*. [23] used a polydimethylsiloxane (PDMS) coating on a toroidal silica micro resonator to enhance its thermal sensitivity. However, combinations of sensitivity improving liquids with micro-resonator devices and sensors results in multiple design challenges, since applying fluids onto the surface of the resonator may lead to poor mechanical stability, the need to protect the fluids from evaporation *etc*. An alternative approach to integration of liquids with WGM resonators is encapsulation of the fluid inside the resonator, fabricated in the shape of a tube, a bubble, or photonic crystal fiber. In this scenario, a thin-walled capillary tube resonators, also referred to as LCORR [31] are especially promising. LCORRs have been used in various sensing applications including the detection of DNA, viruses, proteins and cancer biomarkers [32].

In this manuscript, we propose to enhance the temperature sensitivity of a silica capillary tube resonator with a submicron wall thickness by filling it with a nematic liquid crystal (LC) for thermo-optic tuning applications. The light is evanescently coupled to the resonator using a tapered silica optical fiber. Apart from traditional display applications, LCs are suitable candidates for many photonic applications in which active light manipulation is required. The optical, electrical and magnetic properties of liquid crystals are defined by the orientational order of the constituent anisotropic molecules. The orientational order can be influenced by many factors, such as temperature and electro-magnetic fields. For example, temperature dependence of the refractive indices and optical anisotropy of LCs are often utilized in many LC based tunable devices for various applications [33]. Nematic liquid crystals are attractive temperature tunable materials due to their large negative thermo-optic coefficients and low absorption at the infrared and visible wavelengths. The thermo-optic coefficient of a typical nematic liquid crystal is significantly larger (-9×10^{-4}/°C for 5 CB [34]) than those of many common materials such as deionized water (-0.7×10^{-4}/°C [35]), ethanol (-3.7×10^{-4}/°C [35]), isopropanol (-4×10^{-4}/°C [36]) *etc*. The temperature sensitivity of WGMs excited in nematic liquid crystal droplets embedded in polymer matrix has been demonstrated by Humar *et al.* [37] and recently Y. Wang *et al*. [29] reported thermo-optical tuning of optically pumped WGM lasing emission from dye-doped emulsion microdroplets of cholesteric liquid

Optics EXPRESS

crystals (CLCs) suspended in an aqueous environment. More recently, temperature tuning in a tapered fiber coupled liquid crystal droplet WGM resonator was reported by Y. Wang *et al.* [27]. However, individual LC droplets have never been considered as a tunable optical device. Moreover, in laboratory conditions, evanescent field coupling of light into spherical, bottle or bubble MRs using a fiber taper is typically realized by means of high-resolution 3D micro-positioning stages and optical microscopes for a precise alignment of the tapered fiber waist along the MR equator at a close distance to the resonator surface. Evanescent light coupling is somewhat simpler in the case of cylindrical micro-resonators since only the 2D alignment is necessary. However, in real world applications even the least complex scenario becomes impractical due to the need for bulky and heavy micro-positioning equipment. Therefore, for practical applications development of a simple and reliable packaging method is required for such WGM devices, which would enable their fabrication in a portable and miniature shape without degrading in their laboratory performance. Therefore, in this work we also propose and demonstrate a suitable packaging method for our proposed WGM device. Such a packaged device can be used as a narrow-band thermo-optic tunable filter. The tapered fiber, thin walled silica capillary resonator, and the substrate supporting the resonator, are made from silica, which is good for reducing the temperature expansion imbalance in the packaged device. Additionally, the simplicity, mechanical stability, and the direct interaction of the coupling region with the surroundings (the coupling region is not embedded in a polymer) are the advantages of the proposed packaging technique.

2. Experimental details, results and discussions

2.1. Packaging of the coupled system

The operating principle of the proposed tunable device relies on the interaction between higher order WGMs penetrating into the capillary and the LC inside the capillary whose refractive index is strongly influenced by the applied temperature. In order to increase the efficiency of such interaction, the capillary walls should be sufficiently thin [38]. The thin-walled capillary tube resonator in our experiment was prepared from a short section of a coating-stripped silica capillary tube with inner diameter of 700 μm and outer diameter of 850 μm (Polymicro Technologies). In order to reduce the wall thickness down to the submicron scale, the capillary tube was tapered using a ceramic micro-heater and the fiber pulling setup [39]. Heating and stretching of the capillary tube resulted in the reduction of the capillary wall thickness as well as its external diameter. Resulting external diameter and wall thickness of the uniform tapered portion of the resonator were 41 μm and 0.5 μm respectively. As a first step of the resonator packaging process, the prepared thin-walled capillary tube was attached on to a glass substrate at a height of ~1 mm above the glass surface using a UV- curable glue [Fig. 1(a)]. The total length of the capillary tube was 20 mm.

The tapered optical fiber for light coupling was fabricated using the same fiber pulling setup as for the capillary fabrication and the micro-heater brushing technique described in [39]. The diameter of a uniform waist portion of the fabricated fiber taper was ~1.3 μm. The ends of the tapered fiber were connected to a superluminescent diode (SLD) (Thorlabs) with a wavelength range of 1500–1600 nm and an optical spectrum analyzer (OSA) (Advantest, Q8384) with a resolution of 0.01 nm. To maximize the light coupling efficiency, the uniform tapered portion of the capillary tube acting as the micro-cylinder must be placed perpendicularly and in direct physical contact with the fiber taper waist. Figure 1(b) illustrates schematically the experimental setup for optimizing the coupling efficiency between the fabricated tapered optical fiber and the capillary tube resonator. After achieving the physical contact with the tapered fiber, the capillary tube was slowly moved along the taper axis using a micro-translation stage while maintaining physical contact and a mutually orthogonal orientation. During this process, the transmission spectrum of the taper was observed at the OSA screen to determine the optimal position of the contact point, corresponding to the phase match between the propagating mode of the fiber taper and the fundamental WGM of the

Optics EXPRESS

capillary tube resonator. A manual three-paddle polarization controller (FPC030) placed between the SLD and fiber taper was used to control the polarization and maximize the light coupling efficiency. After achieving the desired WGM spectrum quality, both ends of the tapered fiber were glued to the glass substrate using a UV curable epoxy as shown in Fig. 1(c). The entire packaging process took less than 10 minutes.

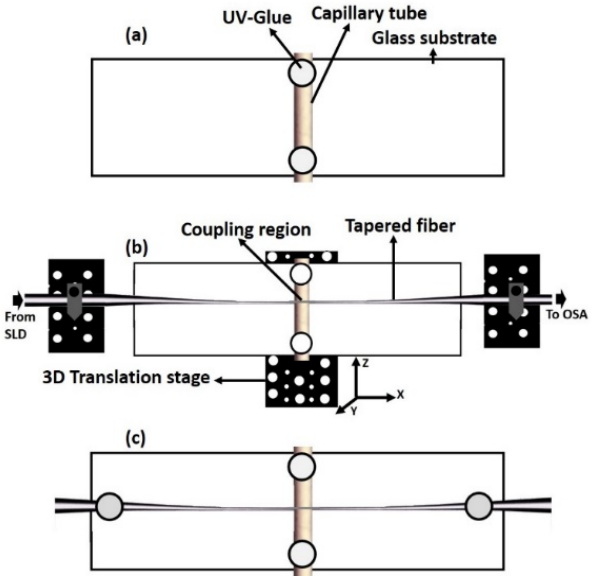

Fig. 1. Schematic of the packaging process: (a) Capillary tube attached to the glass substrate, (b) Maximizing the coupling efficiency between the tapered optical fiber and capillary tube resonator, and (c) Immobilizing the coupled system on a glass substrate.

Robustness of the packaged device was evaluated by observing the effect of vibration on the transmission spectrum. For this test, the packaged sensor was placed on a simple vibration generator driven by a signal generator with a maximum peak-to-peak amplitude of 6 V, as shown in Fig. 2(b). The packaged device was subjected to vibrations at a frequency of 10 Hz for 30 minutes. Spectra of a single WGM resonance dip in the transmission spectrum before and after the vibration test are shown in Fig. 2(a). One can see from the figure that this resonance dip with a central wavelength of 1515.78 nm does not show any changes, and any possible discrepancies are less than the resolution of the OSA employed in the experiment (10 pm).

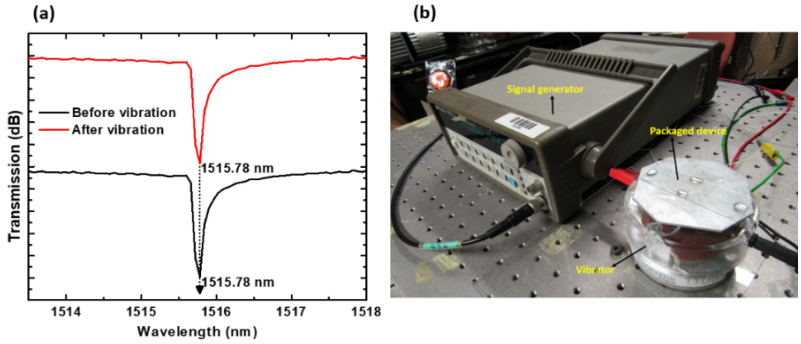

Fig. 2. (a) Selected WGM resonance dip of the packaged device before and after the vibration test. (b) Experimental set up for vibration tests.

Optics EXPRESS

2.2. Thermo-optic tuning experiments using the packaged device

After packaging, the capillary micro-resonator was filled with a nematic liquid crystal (MLC 7012, Licrystal) using a micro-syringe pump. Subsequently both ends of the capillary tube were sealed using a UV curable epoxy. The WGM spectrum experienced dramatic changes due to the significant increase in the effective refractive index inside the resonator. Figure 3 shows the WGM spectra of the packaged capillary tube resonator before and after it was filled with the liquid crystal. One can see from the figure that the average transmission loss of the spectrum, corresponding to the resonator filled with the LC, is much higher. The extinction ratio of the WGM resonances increased from 6 dB to 13 dB (about 60% increase). It should be noted that additional side-lobes appear in the WGM spectra, possibly due to the excitation of non-degenerated WGMs after infiltrating the resonator with higher birefringent LCs. The shift experienced by the WGMs after infiltration is difficult to calculate since the shift is higher than that of the FSR value of the spectrum. The average Q-factor of the highest extinction troughs decreased from ~1.9×10^4 to ~0.9×10^3, suggesting an increased loss within the resonator. The increase in the average loss of the transmission spectrum of the taper after infiltrating the resonator with the LC is probably due to a number of factors such as scattering and absorption of light by the liquid crystal medium. In addition, it can be seen that the free spectral range (FSR) of the WGMs increased for the LC-filled resonator from 11.5 nm to 13.35 nm leading to the reduction of a number WGM resonances observed in the wavelength range from 1500 to 1600 nm.

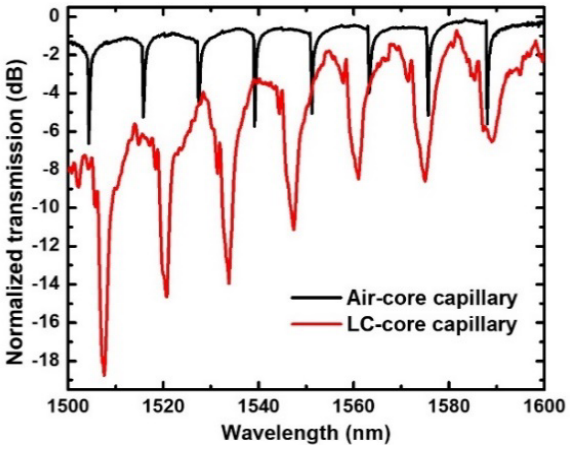

Fig. 3. Experimental WGM spectra of the air core and liquid crystal filled thin-walled micro-capillary.

Analysis of the experimental results allows one to determine and compare the so-called effective diameter of the capillary tube resonator before and after its infiltration with LC, using the approximate equation [40]:

$$D_{eff} = \frac{\lambda^2}{\pi n_{eff} FSR} \tag{1}$$

where λ is the resonance wavelength and n_{eff} is the effective refractive index of the capillary tube resonator.

As can be seen from the above formula, the increase in the effective refractive index of the capillary tube and the increase in experimental FSR due to the infiltration with a higher refractive index LC, should lead to a reduction in the resonator's effective diameter. The notion of effective diameter relates to the localization of WGMs inside the resonator. As was discussed previously by Sumetsky *et al.* in [38] for liquid ring resonator optical sensor

Optics EXPRESS

(LRROS), and in our previous study of the photonic crystal fiber resonators [41], an increase in the effective refractive index of the resonator core leads to the WGMs moving away from the capillary wall toward the higher refractive index core.

In order to demonstrate thermo-optic tuning of the WGM resonances in the fabricated capillary tube resonator we carried out a series of experiments increasing the temperature from room temperature 25°C up to 50°C in 1°C steps by placing the packaged device on a controlled hot stage. Later the temperature was decreased in 1°C steps back to room temperature with all changes in the transmission spectrum recorded using an OSA. The temperature of the hot stage was measured by a thermocouple with 0.1°C measurement resolution. Figure 4 shows the transmission spectra of the packaged LC filled capillary tube resonator with increasing and decreasing temperature in a selected wavelength range. With the increase in temperature, all the WGM resonances experienced monotonic blue shifts and the decrease in temperature resulted in their return back to their initial spectral positions.

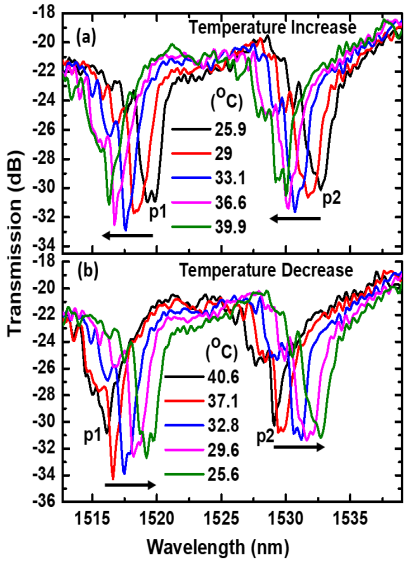

Fig. 4. Transmission spectra of the LC-filled WGM resonator with (a) increasing and (b) decreasing temperature. There is an average spectral shift of 3.23 nm for the temperature change from of 26 to 40 °C.

An average spectral shift of 8.3 nm was observed for the temperature change from of 26°C to 50.8°C with a rate of –270 pm/°C. By way of justification it is well known that both, ordinary and extraordinary refractive indices of nematic LCs depend on the orientational order of the LC molecules. An increase in the LC temperature causes orientational fluctuations leading to the decrease of refractive index of both components [33]. This decrease of the liquid crystal's refractive index leads to the decrease in the WGM resonant wavelengths to satisfy the resonance phase matching condition ($Ln_{eff} = m\lambda_m$, where λ_m is the m^{th} order resonance wavelength, n_{eff} the effective refractive index of the resonator, L is the cavity's round trip length, and m is the integer number of wavelengths along the optical round-trip length termed as the azimuthal mode number) [40].

An increase in temperature also causes a decrease in the Q-factor of the resonance and appearance of additional secondary spectral dips near the main resonance, most likely due to the fact that the liquid crystal core is a birefringent medium and thus has different RIs for different polarizations. The exact position of the resonance minimum was determined by fitting of the primary (highest extinction ratio) spectral trough corresponding to the fundamental mode with Lorentz function. For greater clarity, Fig. 5 illustrates the dip

Optics EXPRESS

wavelength shift of a single WGM resonance [marked p2 in Fig. 4] with increasing and decreasing temperatures in the range from 25.6 to 51°C. The measured wavelength shift (scatter data) is linearly fitted (solid line). Linear fitting of the wavelength response data indicates that the linear regression coefficient is 0.97 for both the temperature increase and temperature decrease cases. The slopes of the linear dependencies are −270 pm/°C (temperature increase) and −265 pm/°C (temperature decrease). The mean value of the slope for the heating and cooling experiments is −267.5 pm/°C. The uncertainty in the slope is calculated as ± 2.5 pm/°C. Thus, the temperature sensitivity of the proposed device is 267.5 ± 2.5 pm/°C. At higher temperatures, the resonance wavelength undergoes stronger fluctuations due to the increasing fluctuations of the hot stage temperature.

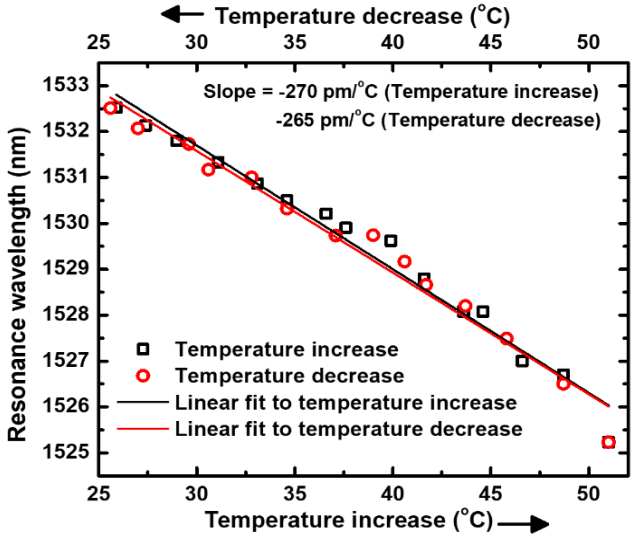

Fig. 5. Spectral shift experienced by a selected WGM resonance [p2 in Fig. 4] with increasing and decreasing temperature.

To test the repeatability of the thermo-optic tuning of the packaged LC filled resonator, two additional experiments were carried out by setting a specific temperature of the hot stage, allowing for a certain time interval to reach the setting and then turning the stage off allowing it to cool down to room temperature. The WGM spectra were recorded continuously and the spectral shift experienced by the modes were analyzed. In the experiment the temperature of the sensor was altered from room temperature (26 °C) to one of two elevated temperatures, 35 °C and 45 °C, by a controlled heating stage.

To understand the evolution of the spectrum as temperature changes with time, the spectral shifts of a selected resonance [marked p2 in Fig. 4] were measured as the temperature was cycled at intervals of 10 minutes between room temperature and an elevated temperature. The WGM spectra of the packaged device were sampled with a fixed time interval of 80 seconds during the experiments. The temperature of the controlled heating stage is monitored using a thermocouple attached to the heater. Figure 6 shows the resonance wavelength plotted against time as the temperature was cycled, for both elevated temperatures. Temperature cycling was repeated for 110 minutes for both elevated temperatures. As can be seen from Fig. 6, the spectral shifts in response to a temperature change are consistent with time. It was found that after temperature cycling of the sensor to an elevated temperature, the resonance wavelength always returned to its room temperature value, with only very minute variations, demonstrating that the sensor is unaffected by repeated temperature cycling. It should be noted that small fluctuations observed in the WGM spectral positions at the constant but elevated temperatures are most likely due to instabilities of the temperature of the hot stage.

Optics EXPRESS

The heater used in the experiments had a maximum instability of ± 1.5°C, measured using a thermocouple attached to its surface.

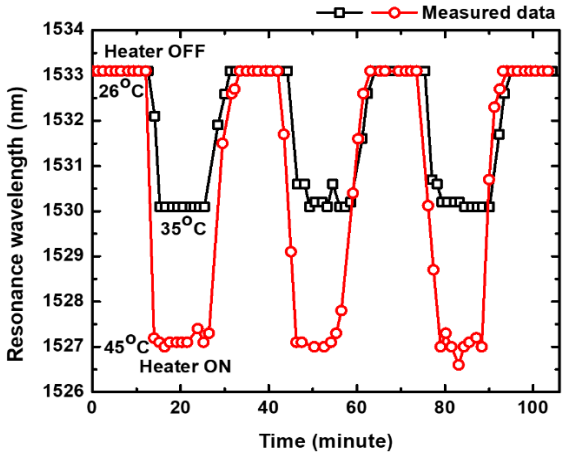

Fig. 6. The resonance wavelength [p2] plotted against time as the temperature was cycled, for elevated temperatures of 35°C and 45°C from room temperature.

In order to obtain better understanding of the role of LC core within the proposed thermo-optic tunable device, we have conducted a set of experiments for characterization of temperature response of an empty (air core) capillary tube resonator, fabricated using the same method and thus with a similar geometry. The temperature was increased from room temperature 31°C up to 47°C with 2°C steps by placing the packaged air-core capillary tube resonator on a temperature controlled hot stage while all changes in the transmission spectrum were recorded using an OSA. The temperature of the hot stage was measured by a thermocouple. Figure 7 illustrates the results of these experiments.

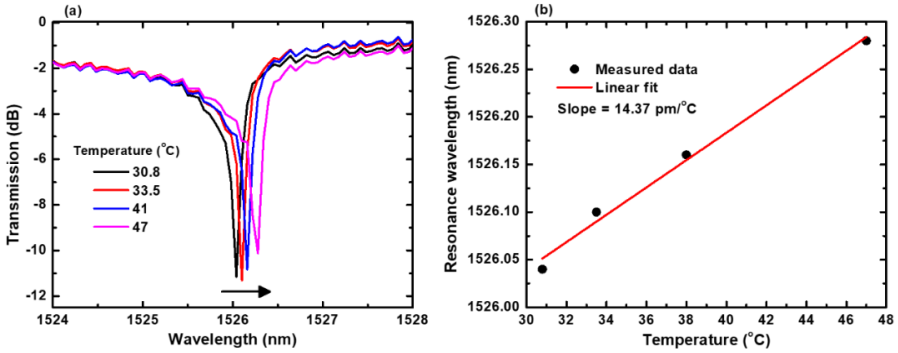

Fig. 7. (a) Selected WGM resonance dip of an air-core capillary tube resonator with increasing temperature. (b) Linear fit of the measured resonance wavelength data with increasing temperature.

As can be seen from Fig. 7(a), the WGM spectrum experiences red shift of 0.24 nm with the increase in temperature, resulting in sensitivity of 14.4 pm/°C. Figure 7(b) shows the linear fit to the measured resonance wavelength shift data with increasing temperature. The redshift of the WGMs with increasing temperature is due to the positive thermo-optic and the thermal expansion coefficients (in the order of ~10^{-5}/°C) of the silica glass [6]. The thermo-optic coefficient of air is even lower than that of the fused silica (~10^{-6}/°C). The sensitivity of

Optics EXPRESS

the air core silica capillary tube resonator is about 19 times lower than that for the LC filled capillary tube resonator.

2.3. Temperature detection limit

The temperature detection limit (DL) of the proposed device can be calculated using the following formula [42]:

$$DL = \frac{R}{S} \tag{2}$$

Here R is the sensor's resolution and S is the sensitivity. The sensor's resolution depends upon the various sources of noise involved in the measurement and determined by the equation [42]:

$$R = 3\sigma\sqrt{\sigma_{ampl-noise}^2 + \sigma_{temp-induced}^2 + \sigma_{spect-res}^2} \tag{3}$$

where σ is the total system noise variance, which can be expressed in terms of all the individual noise variances for amplitude noise ($\sigma_{ampl\text{-}noise}$), temperature induced spectral noise ($\sigma_{temp\text{-}induced}$, and the spectral resolution noise limit ($\sigma_{spect\text{-}res}$). The standard deviation of the amplitude noise can be calculated as [42]:

$$\sigma_{ampl-noise} \approx \frac{\Delta\lambda}{4.5(SNR)^{1/4}} \tag{4}$$

where $\Delta\lambda$ is the full-width half maximum of the mode amplitude derived from the Q factor ($Q = \lambda/\Delta\lambda$). The Q-factor of the LC-filled, and the air-core capillary tube resonators were calculated by fitting the resonance dips with Lorentz equation. The corresponding Q-factors of the selected WGMs of the LC-filled and the air-core capillary tube resonators were 807, and 10263 respectively. We assumed the SNR of the system as 60 dB (equivalent to a ratio of 10^6), then the corresponding $\sigma_{ampl\text{-}noise}$ were calculated as 13.25 and 1.04 respectively for the LC-filled and the air-core capillary tube resonators. We also assumed the standard deviation due to the temperature stabilization ($\sigma_{temp\text{-}induced}$) as 0.01 pm. The spectral resolution of the OSA used in our experiment is 10 pm ± 3%. The error in determining the position of the resonant mode is uniformly distributed between −0.3 pm to + 0.3 pm and the resulting standard deviation of $\sigma_{spect\text{-}res}$ is 0.173 pm. The overall sensor resolutions obtained by Eq. (2) are 39.84 pm and 3.25 pm respectively for the LC-filled and the air-core capillary tube resonators. Then the corresponding temperature DLs can be calculated by Eq. (1) as 0.148°C and 0.23°C respectively for the LC-filled and empty (air core) resonators. From the study it is clear that even though the Q- factor of the LC-filled capillary tube resonator is lower than that for the empty (air core) resonator, the temperature detection limit is slightly better for the LC-filled capillary tube than for the empty one.

Finally, we carried out a comparison of the temperature sensitivity of the proposed tunable device with a number of WGM temperature sensors reported previously, and the results are summarized in Table 1.

As one can see from the Table 1, the device described in this paper offers competitive temperature sensitivity compared to many of the similar WGM devices. Only the dye-doped cholesteric liquid crystal microdroplets [29], DCM-doped oil droplet [28], and the integrated PMMA microsphere resonator [20] show higher temperature sensitivity than the tunable device proposed in this work. It should be noted however that as mentioned in the introduction, individual droplet resonators are difficult to implement as a tunable device due to light coupling and packaging issues. Moreover, the integrated PMMA microsphere sensor described in [20] demands more effort in terms of fabrication and its wavelength tunability range is four times less (1.93 nm) than that of the proposed here tunable device (8.3 nm).

Optics EXPRESS

3. Summary

Table 1. Sensitivity comparison of WGM temperature sensors

Type of sensor	Sensitivity (pm/°C)
Water filled thick (thin) walled fused silica micro-capillary resonator [3]	7.6 (5.4)
Dye-doped hollow polymer optical fiber [25]	11
Water filled thick (thin) walled aluminosilicate capillary micro-resonator [3]	17.2 (13.8)
PMMA wire microcylinder [43]	40.8
PMMA microsphere inserted in a hollow fiber [18]	50
Silica microfiber knot resonator [26]	52
Silicon micro-ring [22]	110
PDMS-coated silica micro-ring [23]	151
Microbubble filled with ethanol [21]	200
Bent optical fiber [24]	212
PDMS microsphere [19]	245
PMMA microfiber knot resonator [26]	266
Tapered optical fiber coupled liquid crystal microdroplet [27]	267.6
Liquid crystal infiltrated LCORR [This work]	**267.5 ± 2.5**
DCM-doped oil droplet [28]	377
Integrated PMMA microsphere [20]	460
Dye-doped cholesteric liquid crystal microdroplets [29]	1500

In summary, thermo-optic tuning of a nematic liquid crystal filled thin-walled silica capillary tube resonator was demonstrated experimentally with a sensitivity of –267.5 ± 2.5 pm/°C. An evanescent field from a tapered optical fiber was used to excite the WGMs in the capillary resonator and record its WGM spectrum in the wavelength range from 1500 to 1600 nm. Fabrication of the tapered fiber and the thin-walled capillary tube was carried out by the micro- heater brushing technique. A simple and robust packaging technique for the proposed tunable device was also developed and demonstrated. Thermo-optic tuning experiments were carried out using the LC filled packaged resonator. An increase in the resonator temperature

Optics EXPRESS

leads to a blue shift of the WGM resonances observed in the transmission spectrum of the fiber taper with a rate of −270 pm/°C and the decrease in temperature resulted in their return back to the initial spectral positions with a rate of −265 pm//°C. The calculated temperature detection limit of the proposed LC filled capillary tube resonator is 0.15°C. The proposed device shows good mechanical stability and repeatability of performance. Initial study indicates that the demonstrated thermo-optic tuning of the WGMs in a nematic liquid crystal thin-walled capillary tube resonator is promising for many photonic applications, for example in tunable filters, switches and sensors.

Funding

Dublin Institute of Technology and DIT Fiosraigh Scholarship Program.

Acknowledgement

Authors would like to acknowledge the support of Dublin Institute of Technology and DIT Fiosraigh Scholarship Program.